

A study of type I X-ray bursts from an NS accreting pure helium

Yan-Cun Ma, He-Lei Liu, Chun-Hua Zhu, Zhao-Jun Wang, Lin Li and Guo-Liang Lü

School of Physics and Technology, Xinjiang University, Urumqi 830046, China; 2274740499@qq.com

Received 2019 August 21; accepted 2019 December 4

Abstract Using the Modules for Experiments in Stellar Astrophysics (MESA) code, we investigate Type I X-ray bursts (XRBs) produced by neutron stars (NSs) accreting pure helium, which are called intermediate XRBs in observations. We simulate 21 models for intermediate XRBs with various mass-accretion rates (\dot{M}) from 2.5×10^{-8} to $5 \times 10^{-10} M_{\odot} \text{yr}^{-1}$. Compared with normal XRBs, in which the NS accretes matter with solar metallicity, intermediate XRBs have higher luminosity and longer recurrence time, which are essentially consistent with observations. We find that the recurrence time of intermediate XRBs is proportional to $\dot{M}^{-2.0}$.

Key words: stars: accretion — star: neutron stars

1 INTRODUCTION

Since the first X-ray bursts (XRBs) were found in a formerly known X-ray source, 4U 1820-30, which were observed by *Astronomische Nederlandse Satelliet* in 1975 (e.g., Bloemendal et al. 1973; Grindlay et al. 1976), thousands of bursts (Meisel et al. 2018) have been observed. These XRBs are divided into two types, type I and type II (Hoffman et al. 1978). The former is associated with unstable nuclear burning on the surfaces of neutron stars (NSs) (e.g., Hanawa et al. 1983; Fujimoto et al. 1987; Koike et al. 1999), while the latter is produced by accretion instability (Parikh et al. 2013). Furthermore, the luminosity of type II XRBs is greater than or equal to $10^4 L_{\odot}$ (Li et al. 2010). In this work, we focus on type I XRBs.

Known X-ray binaries include the accreting NSs in our Galaxy and the Magellanic Clouds, most of which are transients (Li et al. 2010). Low-mass X-ray binaries (LMXBs) are a type of X-ray binary. Due to a loss of orbital angular momentum, mass transfer can occur (Xu et al. 2012). Usually, XRBs are detected in NS LMXBs. There are approximately 200 LMXBs currently known in the Galaxy and the Magellanic Clouds (Liu et al. 2007). Up to now, approximately 111 of them have been observed to produce XRBs (Zand et al. 2018). In these binaries, more than 70% of the NSs' companions are normal stars. This means that the materials accreted by NSs are hydrogen rich. However, approximately 30 of the NS LMXBs may have white dwarfs (WDs) as donors, which are called ultracom-

pact X-ray binaries or their candidates (e.g., Zand et al. 2007; Nelemans et al. 2010; Lü et al. 2017). Ten such cases have been detected in the chemical compositions of WDs, five of which are classified as helium rich (van Haaften et al. 2012). In these systems, XRBs are observed. In the Australia Telescope National Facility database, there are approximately 160 pulsars and WD systems, and approximately 120 systems are composed of pulsars and He WDs (Manchester et al. 2005). Some of them may evolve into ultracompact X-ray binaries, which can produce XRBs that are caused by the release of energy from nuclear reactions.

The chemical composition of He WDs is mainly helium. Therefore, some XRBs are triggered by helium. In fact, based on the duration, luminosity and recurrence time in the observations, XRBs can be divided into three types: normal, intermediate and super XRBs (e.g., Galloway et al. 2017). They are powered by hydrogen enrichment, and helium and carbon ignition. To date, normal XRBs have been observed more than 7000 times, but intermediate and super XRBs have only been identified approximately 70 and 26 times, respectively (Stevens et al. 2014; Galloway et al. 2017). Therefore, most theoretical investigations of XRBs simulate normal XRBs (e.g., Hanawa et al. 1983; Fujimoto et al. 1987; Koike et al. 1999; Woosley et al. 2004). Additionally, super XRBs have been examined in some studies (e.g., Cumming et al. 2001; Brown et al. 2004; Keek et al. 2016).

However, intermediate bursts have seldom been theoretically investigated regarding the relationship between

recurrence time and mass accretion. Keek et al. (2009) performed detailed calculations of intermediate XRBs in order to determine the critical accretion rate for stable helium burning. Zamfir et al. (2014) focused on NSs accreting pure helium and considered how the critical accretion rate for thermonuclear burning stabilizes. Therefore, in their calculations, the mass-accretion rate is very high around, \dot{M}_{Edd} , where $\dot{M}_{\text{Edd}} \sim 1.7 \times 10^{-8} M_{\odot} \text{ yr}^{-1}$ is the Eddington accretion rate of an NS. In this work, we study XRBs produced by an NS accreting pure helium, discuss the differences between them and those produced by an NS accreting hydrogen-rich materials, and find the interval of XRBs as a function of the mass-accretion rate.

In Section 2, we present our assumptions and describe some details of the modeling algorithm. In Section 3, we discuss the main results. In Section 4, the main conclusions are given.

2 MODEL

The Modules for Experiments in Stellar Astrophysics (MESA) code is an open source stellar evolution code that solves the equations of stellar structure and evolution in a completely coupled way (Paxton et al. 2011, 2013, 2015, 2018). It can be employed to study many phenomena of stellar astrophysics, including XRBs. MESA does not simulate the core of an NS, but gives a model of the envelope for a $1.4 M_{\odot}$ NS and offers standard test cases for the models of normal (NS accreting hydrogen-rich materials), intermediate (pure helium) and super (pure carbon) XRBs. We apply the MESA release 10108 for the models of intermediate XRBs. To simulate thermonuclear instability, MESA sets up a model for a $1.4 M_{\odot}$ NS. However, it does not simulate the core of the NS but considers only the bottom of the envelope. For this envelope, the temperature and density range from 2.6×10^7 to 3.5×10^8 K and 1.1×10^{-4} to 1.5×10^8 g cm $^{-3}$, respectively. When thermonuclear runaway occurs, the maximum temperature and density can reach as high as 1.6×10^9 K and 10^9 g cm $^{-3}$, respectively. To describe this envelope, MESA divides it into approximately 1300 levels. We have also divided the envelope into 500 and 2000 levels and obtained the same results.

Based on Zamfir et al. (2014), the critical mass-accretion rate for stable thermonuclear burning of intermediate XRBs is approximately $2\dot{M}_{\text{Edd}}$. In the present paper, we investigate the XRBs. Therefore, we choose a mass accretion rate of less than $2\dot{M}_{\text{Edd}}$ and calculate 21 models in which the mass-accretion rates change from 2.5×10^{-8} to $5 \times 10^{-10} M_{\odot} \text{ yr}^{-1}$. We employ the accreted composition $X(^4\text{He}) = 1$ and apply the nucle-

ar network *approx21_plus_co56.net*. We implement the Ledoux criterion α_{LMT} to express convection. The choices of parameters regarding mixing length theory (α_{LMT}) and semi-convection parameter (α_{SEM}) are 1.6 and 1.0, respectively.

3 RESULTS

3.1 Comparison with Normal XRBs

For a comparison, we also simulate normal XRBs in which the chemical compositions of materials accreted by an NS are similar to the solar composition. In observations, the duration of normal XRBs is approximately between 10 and 100 s, while it is approximately between several minutes and several hours for intermediate XRBs. The recurrence time for the former is approximately several hours to several days, but it is approximately several weeks or months for the latter. The luminosities of normal XRBs are approximately between 10^2 and $10^5 L_{\odot}$, but intermediate XRBs are usually approximately 10 times more luminous.

Figure 1 shows the light curve of normal and intermediate XRBs with a certain mass-accretion rate of $2.0 \times 10^{-9} M_{\odot} \text{ yr}^{-1}$. The results simulated in the present paper are within the scope of observations. Compared with normal XRBs, in our simulation, the luminosities of the intermediate XRBs are higher, and the duration and recurrence times are longer. The main reason is as follows: Helium burning requires higher temperature and pressure than does hydrogen burning. Therefore, an NS must accrete more mass for intermediate XRBs.

The nuclear physics processes are very complex for XRBs (e.g., Woosley et al. 1976; Fisker et al. 2008; Woosley et al. 2004). Any XRB may involve charged particle reactions that can create isotopes with masses of up to $A = 100$. The relevant types of reaction sequences in XRBs include *rp*- and *αp* - processes (e.g., Wallace et al. 1981; Schatz et al. 2006). In this work, we do not discuss the nuclear reactions in particular but give only two dominant nuclear reactions, which mainly power the luminosity. Figure 2 indicates that the energy of normal XRBs is produced mainly by hydrogen and neon burning, and that of intermediate XRBs comes from helium and neon burning.

3.2 Intermediate XRBs

Based on the theory and observations, the duration, recurrence time and luminosity of XRBs are strongly related to the mass-accretion rate. The model of stellar evolution is based on massive star core collapse; most of the material falls on the NS and forms an accretion disk to cause the change in mass accretion (Li et al. 2003). For nor-

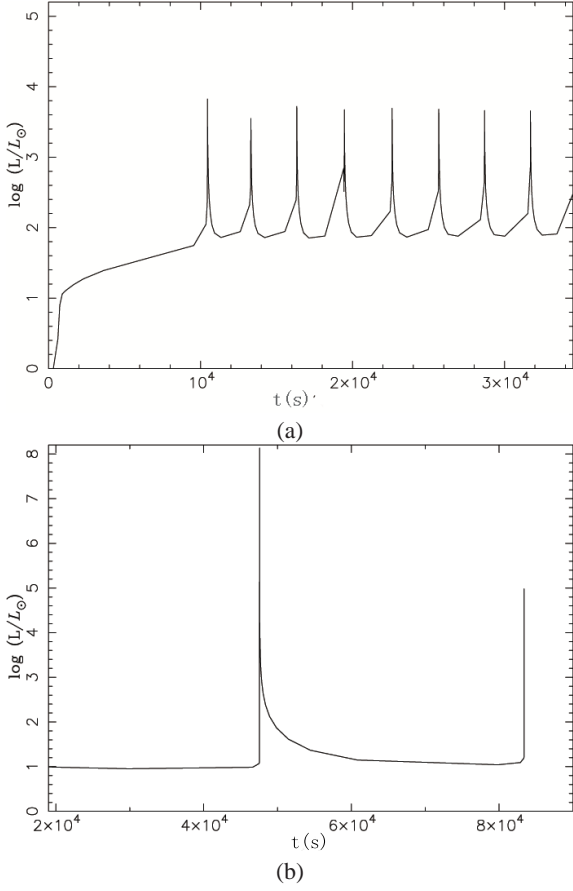


Fig. 1 The light curve of XRBs for models with $\dot{M} = 2.0 \times 10^{-9} M_{\odot} \text{ yr}^{-1}$. Panels (a) and (b) are for models of normal and intermediate XRBs, respectively.

mal XRBs, analyzing 24 normal bursts from GS 1826-24 as observed by the *Rossi X-Ray Timing Explorer* and assuming that the mass-accretion rate \dot{M} is linearly proportional to the observed X-ray luminosity, Galloway et al. (2004) found that the recurrence time equals approximately $\dot{M}^{-1.05 \pm 0.02}$. However, Keek et al. (2010) ascertained that the recurrence time of EXO 0748–676 is a bimodal distribution.

Recently, according to whether the recurrence time since the previous burst was shorter or longer than 45 minutes, Keek et al. (2017) divided the recurrence times into two types: short and long recurrence times. They asserted that the former is produced by unburned hydrogen during a long recurrence-time burst with mixing down to the ignition depth by convection for several minutes. Very recently, Wang et al. (2017) stated that normal XRBs may be governed by a self-organized criticality process.

Compared to more than 7000 normal XRBs observed, approximately only 70 intermediate XRBs have been detected. Therefore, we do not know whether the recurrence time of intermediate XRBs is also a bimodal distribution.

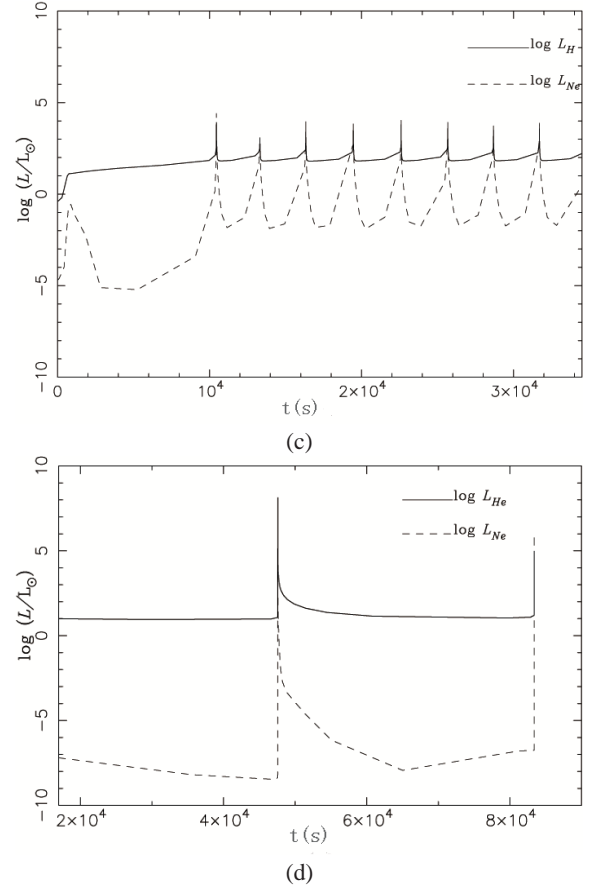


Fig. 2 Similar to Fig. 1, but for luminosity powered by different nuclear reactions. L_H , L_{He} and L_{Ne} represent the luminosity released by hydrogen, helium and neon burning, respectively.

In this work, we discuss the relationship between the mass-accretion rate and the recurrence time. In addition, we give the relations between mass-accretion rate and critical mass.

Figure 3 displays the luminosities of several intermediate XRBs with mass-accretion rates of $2.5 \times 10^{-8} M_{\odot} \text{ yr}^{-1}$, $5 \times 10^{-9} M_{\odot} \text{ yr}^{-1}$ and $5 \times 10^{-10} M_{\odot} \text{ yr}^{-1}$. The lower the mass-accretion rate is, the higher the luminosity is, but the longer the recurrence is. These trends are consistent with observations.

In this research, we simulate 21 models for intermediate XRBs with various mass-accretion rates from 2.5×10^{-8} to $5 \times 10^{-10} M_{\odot} \text{ yr}^{-1}$. Figure 4 gives the mass-accretion rates and recurrence times in 21 models. The correlation coefficient equals 0.99. Generally, the results are consistent with a coefficient of approximately 1. Using the least-squares method, we fit the function between the mass-accretion rates and recurrence times (Δt_{rec}) by

$$\Delta t_{\text{rec}} = 10^2 \left(\frac{\dot{M}}{10^{-10} M_{\odot} \text{ yr}^{-1}} \right)^{-2.0} \text{ d}. \quad (1)$$

The above relation for the intermediate XRBs is different from the relation of $\Delta t_{\text{rec}} \sim \dot{M}^{-1.05 \pm 0.02}$ proposed by

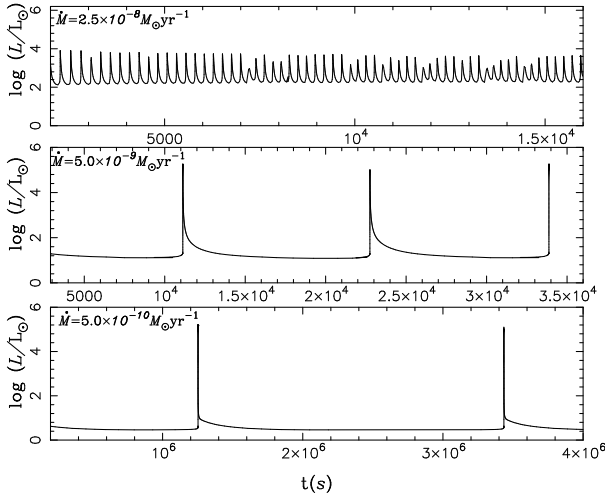


Fig. 3 The light curve of intermediate XRBs with mass-accretion rates of 2.5×10^{-8} , 5×10^{-9} and $5 \times 10^{-10} M_{\odot} \text{ yr}^{-1}$.

Galloway et al. (2004) for normal XRBs. In LMXBs, the mass-accretion rates can be estimated by the X-ray luminosity by $\dot{M} = L_X/(\eta c^2)$, where L_X and c are the X-ray luminosity and speed of light, respectively. The parameter $\eta \sim 0.1$ is the efficiency of converting the accreted mass into X-ray photons. In addition, Δt_{rec} can be obtained by observing the interval of two contiguous XRBs. In principle, we can check the relation of Equation (1). Unfortunately, only 70 intermediate XRBs have been identified, and most of the observed intermediate XRBs occurred after normal XRBs. Although intermediate XRBs have been observed from 4U 0614+091, SLX 1735–269, 4U 1820–30 and 4U 1850–086, their recurrence time was not observed (Serino et al. 2016). Kuulkers et al. (2010) suggested that the recurrence time of 4U 0641+091 is 155 d at a mass-accretion rate of $10^{-10} M_{\odot} \text{ yr}^{-1}$, which is consistent with Equation (1). Therefore, we need more observations to check Equation (1).

4 CONCLUSIONS

In this work, we investigate intermediate XRBs, in which NSs accrete pure helium. Compared with normal XRBs powered by thermonuclear runaway of the CNO cycle and neon burning, the intermediate XRBs are triggered by the triple-alpha process and neon burning. The luminosity of the intermediate XRBs is higher than that of normal XRBs with the same mass-accretion rate. Similarly, the duration and recurrence times of the former are longer than those of the latter. We find that a relation between the mass-accretion rates and recurrence times can be given by $\Delta t_{\text{rec}} = 10^2 \left(\frac{\dot{M}}{10^{-10} M_{\odot} \text{ yr}^{-1}} \right)^{-2.0} \text{ d}$. However, we need more observations to verify this conclusion.

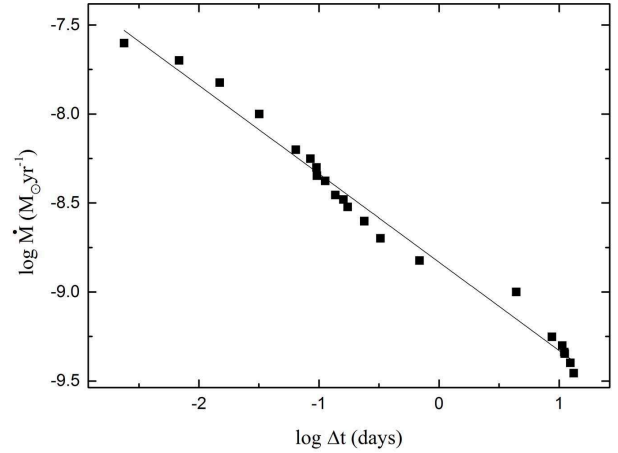


Fig. 4 The fitting function of the mass-accretion rates and the recurrence times of intermediate XRBs. *Solid squares* represent the 21 models simulated in this work.

Acknowledgements This work received generous support from the National Natural Science Foundation of China (Grant Nos. 11763007, 11473024, 11463005, 11863005, 11803026 and 11503008). We would also like to express our gratitude to the Tianshan Youth Project of Xinjiang (Grant No. 2017Q014).

References

- Bloemendal, W., & Kramer, C. 1973, Philips Technical Review, 33, 117
- Brown, E. F. 2004, ApJ, 614, 57
- Cumming, A., & Bildsten, L. 2001, ApJ, 559, 127
- Fujimoto, M. Y., Sztajno, M., Lewin, W. H. G., & van Paradijs, J. 1987, ApJ, 319, 902
- Fisker, J. L., Schatz, H., & Thielemann, F.-K. 2008, ApJS, 174, 261
- Grindlay, J., Gursky, H., Schnopper, H., et al. 1976, ApJ, 205, L127
- Galloway, D. K., & Keek, L. 2017, arXiv:1712.06227
- Galloway, D. K., Cumming, A., Kuulkers, E., et al. 2004, ApJ, 601, 466
- Hoffman, J. A., Marshall, H. L., & Lewin, W. H. G. 1978, Nature, 271, 630
- Hanawa, T., Sugimoto, D., & Hashimoto, M.-A. 1983, PASJ, 35, 491
- in't Zand J. J. M., Jonker P. G., Markwardt C. B. 2007, A&A, 465, 953
- Koike, O., Hashimoto, M., Arai, K., & Wanajo, S. 1987, A&A, 342, 464
- Keek, L., & Heger, A. 2016, MNRAS, 456, 11
- Keek, L., Langer, N., & in't Zand, J. J. M. 2016, A&A, 502, 871
- Keek, L., Galloway, D. K., in't Zand, J. J. M., & Heger, A. 2010, ApJ, 718, 292

- Keek, L., & Heger, A. 2017, *ApJ*, 842, 113
- Kuulkers, E., in 't Zand, J. J. M., Atteia, J.-L., et al. 2010, *A&A*, 514, 65
- Lü, G., Zhu, C., Wang, Z., & Iminniyaz, H. 2017, *ApJ*, 847, 62
- Li, T., & Li, X.-D. 2010, *RAA (Research in Astronomy and Astrophysics)*, 10, 672
- Li, X.-D. 2003, *ApJ*, 596, 199
- Liu, Q. Z., van Paradijs, J., & van den Heuvel, E. P. J. 2007, *A&A*, 469, 807
- Manchester, R. N., Hobbs, G. B., Teoh, A., & Hobbs, M. 2005, *AJ*, 129, 1993
- Meisel, Z., Deibel, A., Keek, L., et al. 2018, *Journal of Physics G Nuclear Physics*, 45, 093001
- Nelemans, G., Yungelson, L. R., van der Sluys, M. V., & Tout, C. A. 2010, *MNRAS*, 401, 1347
- Parikh, A., José, J., Sala, G., & Iliadis, C. 2013 *Progress in Particle and Nuclear Physics*, 69, 225
- Paxton, B., Bildsten, L., Dotter, A., et al. 2011, *ApJS*, 192, 3
- Paxton, B., Cantiello, M., Arras, P., et al. 2013, *ApJS*, 208, 4
- Paxton, B., Marchant, P., Schwab, J., et al. 2015, *ApJS*, 220, 15
- Paxton, B., Schwab, J., Bauer, E. B., et al. 2018, *ApJ*, 234, 34
- Stevens, B. L., Ries, J. G., Dupouy, P., et al. 2017, *Minor Planet Electronic Circulars*, 2014-Y97
- Schatz, H., Bildsten, L., Cumming, A., & Wiescher, M. 1999, *ApJ*, 524, 1014
- Schatz, H. 2006, *Proceedings of the International Symposium on Nuclear Astrophysics - Nuclei in the Cosmos - IX. 25-30 June 2006*, 2.1
- Serino, M., Iwakiri, W., Tamagawa, T., et al. 2016, *PASJ*, 68, 95
- van Haften, L. M., Voss, R., & Nelemans, G. 2012, *A&A*, 543, A121
- Wang, J. S., Wang, F. Y., & Dai, Z. G. 2017, *MNRAS*, 471, 2517
- Woosley, S. E., & Taam, R. E. 1976, *Nature*, 263, 101
- Wallace, R. K. 1981, *ApJS*, 45, 389
- Woosley, S. E., Heger, A., Cumming, A., et al. 2004, *arXiv:0307425*
- Xu, Q., Li, T., & Li, X.-D. 2012, *RAA (Research in Astronomy and Astrophysics)*, 12, 1417
- Zamfir, M., Cumming, A., & Niquette, C. 2014, *MNRAS*, 445, 3278
- Zand, R., Camsari, K. Y., Datta, S., & DeMara, R. F. 2018, *arXiv:1811.11390*